Journal of Structural Geology, Vol. 14, No. 4, pp. 381 to 394, 1992
Printed in Great Britain

0191-8141/92 \$05.00+0.00

Modes of superposed buckling in single layers controlled by initial tightness of early folds

S. K. GHOSH, N. MANDAL, D. KHAN and S. K. DEB

Department of Geological Sciences, Jadavpur University, Calcutta 700 032, India

(*Received* 1 *May* 1991; *accepted in revised form* 4 *November* 1991)

Abstract—In a series of experiments with soft test models, superposed buckling folds were produced in a competent layer resting on a slab of incompetent painter's putty. The angle between the hinge lines of the first set of cylindrical folds (F_1) and the direction of the second compression (P_2) was varied in the different experiments. The experiments showed that with an increase in the initial tightness of F_1 there was a transition from one mode of superposed buckling to another. When the interlimb angle of F_1 was very large the superposed deformation gave rise to a dome-and-basin pattern (the first mode of superposed buckling). The second mode, with small F_2 folds riding over larger F_1 folds, developed when the initial interlimb angle ranged roughly between 135° and 90°. The third mode was observed when the F_1 interlimb angle was less than about 90° but the fold was not very tight. In the third mode a set of non-plane non-cylindrical folds developed; however, the sinuous hinge line of the non-cylindrical structure was newly created by replacing the old F_1 hinge. When F_1 was very tight or isoclinal the fourth mode of superposed buckling led to the development of non-plane non-cylindrical folds without concomitant hinge replacement.

INTRODUCTION

ONE OF the major problems of superposed folds is the following: can we predict the geometry of the superposed folds if the shape and orientation of the first folds in a layer are given and the nature of bulk deformation is known? This problem has been discussed in detail by Ramsay (1967) and Ramsay & Huber (1987) in terms of the model of shear folding. In contrast, there are very few detailed studies of the morphology of folds produced by superposed buckling. Although fold interference patterns were classified by Ramsay in terms of heterogeneous shear, such interference patterns may also develop during superposed buckle-folding; however, the mechanics of development of such interfering buckle-folds is not properly understood as yet (Ramsay & Huber 1987, pp. 489 and 493).

Both field studies and experiments show that superposed buckling may give rise to interfering folds morphologically similar to any one of the four major classes of fold interference patterns of Ramsay: (a) type 0, with an overall plane cylindrical geometry; (b) type 1, with a plane non-cylindrical shape; (c) type 2, with a non-plane non-cylindrical shape; and (d) type 3, with non-plane cylindrical geometry. Experiments on superposed buckling (Ghosh & Ramberg 1968, Skjernaa 1975, Watkinson 1981) further indicated that when an early generation of folds is subjected to a hinge-parallel shortening there may be two situations. In one of these, superposed buckling produces a type 1 interference. In the other situation, the later folds develop by deformation of the axial planes and hinges of the early folds and give rise to a type 2 interference. The type 1 interference was produced when the early set of folds was open while the type 2 interference developed when the early folds were tight or isoclinal. A similar contrast in the modes of superposed buckling was reported by Julivert & Marcos (1973, p. 374) from the Cantabrian zone of north-west Spain, where gentle folds were refolded into domes and basins but the tight folds were deformed to non-plane non-cyclindrical shapes. Watkinson (1981) has shown from Douarnenez Bay, Brittany, that a type 2 interference has developed by refolding of very tight early folds with narrow hinge zones while there has been a superposition of smaller folds in a type 1 interference pattern where the early folds have rounded hinges. The smaller folds are similar to the small second generation folds which ride over the hinges of early folds in the experiments of Ghosh & Ramberg (1968). The experiments by Ghosh & Ramberg (1968) further showed that a later generation of folds did not develop if the angle between the early fold hinge and the direction of later compression was more than 30°.

In the next section we present a new series of experiments, similar to those by Ghosh & Ramberg (1968), but with varying tightnesses of the early folds, and with different angles between the early fold hinge and the later direction of shortening. In addition to the rotation and tightening of the early folds in certain situations, we recognized from these experiments four distinct modes of superposed buckling. The experiments indicated that the mode of superposed buckling depends to a great extent on the initial shape of the early folds.

EXPERIMENTAL METHODS

The experiments were carried out in a pure shear apparatus (Fig. 1) in which the maximum shortening could be achieved in a horizontal direction and the model was free to extend in a vertical direction. To reduce friction the basal plate of the apparatus on which the model was placed was lubricated with gear oil and

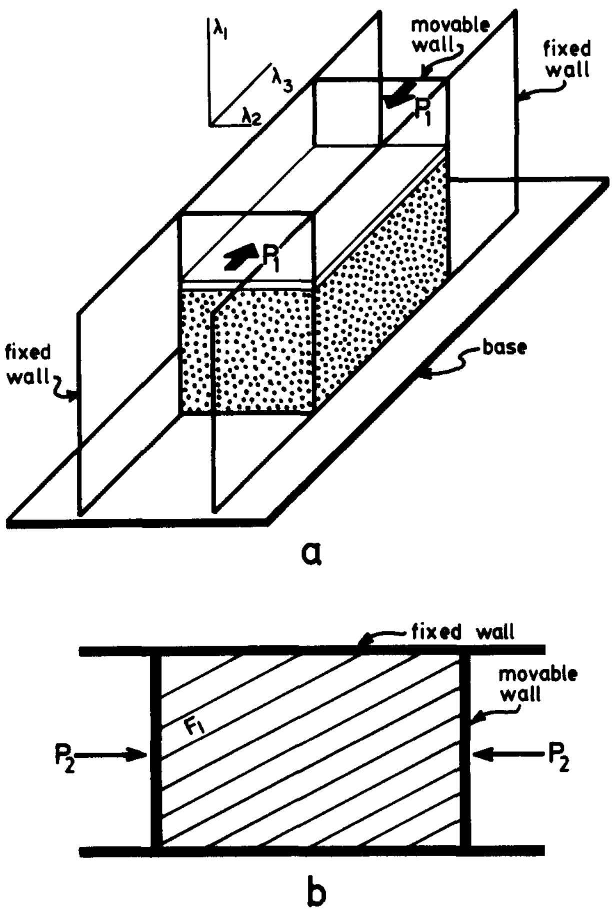

Fig. 1. (a) Horizontal sheet of modelling clay resting on a slab of painter's putty. The model is subjected to a pure shear. (b) The model is deformed by pure shear with the layer in horizontal attitude. The angle between the first fold axis (F_1) and the direction of the second compression (P_2) was varied in the different experiments.

the inside faces of the vertical confining walls were lubricated with liquid detergent.

The superposed folds in the experiments were produced in a single layer of modelling clay of 1, 2 or 3 mm thickness. In some of the models the 'layer' consisted of two layers of modelling clay with a greased interface. A total of 68 experiments were carried out. In only two of these (Table 1) the layer was placed between two thick slabs of painter's putty. In all the other models the layer was placed on top of a slab of painter's putty.

Table 1. Summary of experimental results

Interlimb angle (°)	Number of experiments $\theta = 0$ $\alpha = 0$	$\theta \neq 0$ $\alpha = 0$	$\theta = 0$ α = 10–20°	Mode
165–155	5(2)	5		1
155–145	5(2)	2		1
145–135	5(2)	2		1
135–125	5			2,1
125–115	3	3	2	2
115–90	3[1]		2	2
90–70	3			3,2
70–50	7[1]	3	1	3
50–30	5			3
30–20	4	1		4
20–0	2			4

Figures in parentheses indicate the number of experiments with artificially induced $F1$ folds. Figures in brackets indicate the number of experiments with an embedded layer.

For convenience of description the set of first generation folds will be described here as F_1 and the superposed folds produced in the second deformation will be designated F_2. The directions of bulk shortening in the first and the second deformations will be described as P_1 and P_2. In the majority of experiments the F_1 folds were produced by starting with a straight layer and by deforming the model by a layer-parallel shortening. The central part of the model, where the folds were more or less uniformly developed, was then cut out and this part was used for the second deformation to generate the superposed folds. In six experiments the F_1 folds were artificially induced. In all these six models the F_1 folds were gentle, with interlimb angles ranging from 135° to 165° (see Table 1).

The artificially induced F_1 folds were produced in the following manner. After rolling out a thin sheet of modelling clay, a thin strip of about 1.5 cm width was cut out from its edge. The strip was placed on a thick slab of painter's putty along one of its edges and was lightly pressed down with a glass plate so that the strip stuck firmly with the putty surface. The slab of putty was then shortened parallel to the length of the strip of modelling clay to produce a set of gentle folds. The profile of the folds along the interface of the modelling clay and putty was drawn on a transparent sheet for that segment in which the folds were regular, had more or less similar wavelengths and had the desired interlimb angle. This fold-form was then drawn on two strips of cardboard in the form of a train of more or less periodic waves. The fold-form on the cardboard strips was cut out so that one side of each strip showed the wavy form. The two strips of cardboard were held along two opposite faces of a rectangular slab of putty and a wavy surface was cut out near its top surface by drawing a stretched sitar wire guided along the wavy edges of the cardboards. A sheet of modelling clay was placed over this wavy surface of putty by gradually lowering it from one side and lightly pressing it down with fingers.

Before placing the model in the pure shear apparatus the vertical side-walls of the model were coated with a 1.5 cm thick layer of putty so that the folded layer of modelling clay would not remain in contact with the confining walls of the apparatus. Let the trend of the F_1 axis with reference to the direction of P_2 be the angle θ and let the dip of the enveloping surface of the F_1 folds be α. When $\alpha \neq 0$, the dip is always towards the direction of P_2. In the majority of the models (see Table 1) the enveloping surface of the F_1 folds was kept horizontal and the axis of the F_1 folds was parallel to the shortening direction (P_2) of the second deformation. In other words, in the majority of cases $\theta = 0$ and $\alpha = 0$. In some of the experiments the enveloping surface of F_1 was kept horizontal ($\alpha = 0$) but the F_1 axis was at an angle to P_2 ($\theta \neq 0$). In a small number of experiments (Table 1) the enveloping surface was inclined and the F_1 axis was at an angle to P_2 ($\theta = 0$, $\alpha \neq 0$), the angle of inclination, α, being equal to the angle between P_2 and the F_1 axis.

Except for two, all the experiments were carried out with the same type of modelling clay and the same type of putty. In one experiment the contrast in competence was increased by using a stiffer modelling clay and a softer putty. In another experiment the contrast was reduced by mixing a small amount of modelling clay with putty.

FIRST MODE OF SUPERPOSED BUCKLING

P_2 *at a right angle to* P_1 ($\theta = 0, \alpha = 0$)

The first mode of superposed buckling gave rise to a dome-and-basin pattern and was seen only when F_1 was very open (with interlimb angle greater than about 135°) and the curvature at its hinge was quite small (Figs. 2a & b). The trends of the F_1 and F_2 folds in these models are discernible by joining the crest points of the adjoining domes in the two directions. When F_1 and F_2 have more or less the same tightness and have approximately the same curvature, a distinct hinge line is not recognizable over the domes and basins. When the F_2 folds become tight their curved hinge lines become distinct. The curvature of the F_2 hinge line increases with progressive tightening of the folds. Morphologically, the resulting structure is a type 1 fold interference. When the F_2 folds become very tight or isoclinal, the F_1 hinges cannot be distinguished at all and the F_1 folds can only be seen by the wavy form of the F_2 hinges. In the first mode of superposed buckling the F_2 folds can be very tight while the F_1 folds are still quite open. On the other hand, a set of open F_2 folds superposed on tight F_1 folds never develops in the first mode of superposed buckling. In the course of tightening of the F_2 folds and with a progressive accentuation of their hinge line curvatures, the amplitude of F_1 also increases, although there is no change in F_1 fold wavelength (Fig. 6). Thus, when the hinge line curvatures of F_2 have greatly increased, the F_1 folds may also show a significant increase in their amplitude/wavelength ratio.

P_2 *oblique to* P_1

A dome-and-basin pattern also developed when F_1 and F_2 were oblique to each other (Figs. 2c & d and 3a), with $\alpha = 0, \theta \neq 0$. In the experiments in which F_1 was very open (with interlimb angle greater than 135°) the dome-and-basin structure developed even when the direction of the second compression P_2 was at an angle of 50° with the F_1 hinges. A set of new fold hinges did not develop when the angle between F_1 and P_2 was larger than 50°; instead, the F_1 folds were progressively tightened and rotated during the second deformation. Although the F_1 folds remained more or less cylindrical and with planar axial surfaces, their shapes and orientations were considerably modified (Fig. 7). Since the final shape and orientation of the folds were a result of the two superposed deformations, they should be distinguished from the F_1 folds; perhaps Ramsay & Huber's (1987, p. 493) concept of redundant superposition (type 0 interference) may be extended to include this type of structure.

When the angle between P_2 and F_1 is rather small ($\alpha = 0, \theta = 20$–$30°$) and both sets of folds in the experiments are open, the domes and basins are usually elongate and are aligned in a step-like pattern. The two sets of lines obtained by connecting the adjoining crests (antiform–antiform intersections) or the adjoining troughs (synform–synform intersections) are initially perpendicular to P_1 and P_2. With progressive deformation the lines, such as CC′ (Fig. 8a), perpendicular to P_2 do not rotate, but the other set of lines parallel to DD′ does rotate so that the two sets of lines make progressively lower angles with each other. In the general situation the long directions of the oval outcrops of elongate domes and basins on a horizontal section do not coincide with either CC′ or DD′ (Figs. 3b and 8b). These oblique domes and basins are very similar to those described in map-scale by de Sitter (1952) from the Atlas Mountains in Morocco. There, the oblique domes and basins have formed by the intersection of earlier NE-trending folds with E–W-trending later folds. de Sitter suggested that the angle between the early and the late sets of folds was reduced during the later deformation. Even when the experimental F_2 folds have the same tightness as F_1 and both sets of folds are very gentle, the domes and basins have a distinct linear trend. This is because the intercept of an F_2 fold on an F_1 fold (line AB in Fig. 8c) is larger than the wavelength (line AC) of F_1. With progressive tightening of the F_2 folds the long direction of the oval outcrops of the domes and basins become subparallel to CC′ of Fig. 8(a). This process is accompanied by progressive rotation of the F_1 hinges, resulting in a decrease in the angle between F_1 and F_2 axes and a progressive tightening of the F_1 folds.

SECOND MODE OF SUPERPOSED BUCKLING

P_2 *at a right angle to* P_1 ($\theta = 0, \alpha = 0$)

When the F_1 folds were moderately tight the first mode of superposed buckling was inhibited and was replaced by another mode. If the initial interlimb angle of F_1 ranged between 90° and 135°, the second deformation gave rise to a set of folds riding across the hinges of the first generation folds (Fig. 4a). The arc-lengths of the F_2 folds are distinctly smaller than those of the F_1 folds (Ghosh & Ramberg 1968). This mode of buckling is similar to the symmetrical buckling of a cylindrical shell under the action of an axial compression (Timoshenko & Gere 1961, pp. 457–462). The initial wavelength of the F_2 folds decreases with an increase in curvature at the hinge zone of F_1. When F_1 and F_2 are orthogonal, the F_2 folds are plane non-cylindrical. In the second mode of superposed buckling with F_1 at right angles to F_2, the limbs and the hinges of the F_1 folds are locally distorted, but there is no significant change in the trend of F_1 and in the attitude of its axial planes (Fig. 9a).

In sections which intersect both F_1 and F_2 hinges, the outcrops have an oval shape characteristic of the type 1 interference (Fig. 9b).

P_2 *oblique to* P_1

When P_1 and P_2 are oblique (Figs. 4b and 10), either with $\alpha = 0$, $\theta \neq 0$, or with P_2 inclined to the overall orientation of the layer ($\theta = 0$, $\alpha = 10$–$20°$), the angle between the F_1 and F_2 hinge lines is variable and the axial surface of a non-cylindrical F_2 fold may not be parallel in all places. In other words, the F_2 folds may be non-plane. Moreover, because of the oblique superposition, the initial hinge angle (Williams & Chapman 1979) of a smaller F_2 fold (or the radius of curvature of its arcuate hinge line) will be smaller than the interlimb angle (or the radius of curvature) of the folded surface of F_1 (Fig. 10). With progressive tightening the axial surfaces of F_2 become more or less planar. Although, in the second mode of superposed buckling, the oblique superposition of small F_2 folds on large F_1 folds (either with $\theta \neq 0$, $\alpha = 0$ or with $\theta = 0$, $\alpha \neq 0$) causes only localized distortions in the shape of F_1, without an overall bending of its axial planes, the general orientations of the F_1 hinge lines and axial planes change in the course of progressive deformation, so that the F_1 hinge lines make a smaller angle with the XY plane of the second deformation.

The second mode of superposed buckling may give rise to a variety of outcrop patterns (Figs. 4c and 11), such as (a) symmetrical or asymmetrical closed oval outcrops (Fig. 11a), (b) symmetrical or asymmetrical closed triangular outcrops (Fig. 11b), (c) three-pronged outcrops (Figs. 11c & d) and (d) mushroom-shaped outcrops (Fig. 11e). The first three patterns are generally produced when both F_1 and F_2 have planar axial surfaces. The mushroom-shaped pattern forms when, in oblique superposition, the F_2 axial surface is differently oriented on different parts of the F_1 fold.

THIRD MODE OF SUPERPOSED BUCKLING

This mode of superposed buckling was seen when the F_1 folds were fairly tight (with limb dips less than about 90°) but not very tight or isoclinal (Fig. 5). The third mode of superposed buckling develops when the curvature of the folded surface at the F_1 hinge zone is moderately large, but when the F_1 hinge is not sharp and the hinge zone is not too narrow. In this mode of superposed buckling in a single-layer, the F_1 and the F_2 folds are roughly of the same size and the total structure has a non-plane non-cylindrical geometry. To describe the characteristic morphology of these superposed folds let us assume, as we have in the experiments, that the general orientation of the layering is subhorizontal. In the third mode of superposed buckling the F_2 folds then plunge in opposite directions on the two limbs of an F_1 fold, with an antiformal F_2 on one limb of F_1 passing to a synformal F_2 on the other limb (Ghosh & Ramberg 1968). This mode of superposed buckling is characterized by the following morphological features.

(a) Each F_2 fold (either an antiform or a synform) occupies a roughly triangular area (cf. Ghosh & Ramberg 1968, fig. 9). An antiformal F_2 has a relatively wide span in the neighbourhood of the F_1 antiformal hinge and it narrows down at the F_1 synformal hinge. Similarly, a synformal F_2 has a relatively wide span near a synformal F_1 hinge and it tapers towards an antiformal F_1 hinge (Fig. 12a).

(b) The initiation of the F_2 folds is associated with replacement of the old F_1 hinge lines by sinuous new hinge lines. A material line which was once parallel to a straight F_1 hinge line now appears as a gently sinuous or more or less straight line (dark line in Figs. 5a & b and dashed line in Fig. 12b) at an angle with the strongly sinuous newly created hinge line. With progressive tightening during the second deformation the hinges of the F_2 synforms propagate across the F_1 synformal hinges. At a point where a synformal F_2 propagates across an antiformal F_1 the initial upward convexity of the layer changes to an upward concavity (Fig. 12c).

Although the total structure resulting from the third mode of superposed buckling is morphologically similar to that of type 2 fold interference (Ramsay 1967, p. 525), what appears to be a strongly curved F_1 hinge is in reality a feature that is newly created during the second deformation. These sinuous hinge lines, however, are quite distinct from the hinge lines of the F_2 folds whose axial surfaces are more or less orthogonal to P_2. The process of development of the new sinuous hinge lines by obliterating the earlier F_1 hinge lines is described here as hinge replacement. The recognition of the process of hinge replacement gives rise to a problem of nomenclature. The new sinuous hinge line cannot be referred to either as F_1 or as F_2. In the following description it will be designated F_1' since it replaces the F_1 hinge line and has morphological similarity with the hinge line of an early fold. Hinge replacement is a characteristic feature of the third mode of superposed buckling. As a consequence of hinge replacement, a lineation parallel to F_1 will be oblique to F_1'. The hinge replacement is a continuous process during the second deformation. During progressive deformation the position of an F_1' hinge line changes continuously through successive material lines. However, once the axial surfaces of F_1' have rotated to the field of extension, both the F_1' and the F_2 folds are simultaneously tightened. Beyond a certain stage of tightening the hinge lines of the F_1' folds continue to coincide with a single material line.

FOURTH MODE OF SUPERPOSED BUCKLING

Superposed buckling by a shortening along the axis of very tight or isoclinal F_1 folds, and having a very large curvature of the folded surfaces at the hinges, invariably produced in the experiments a type 2 interference with curved hinge lines and curved axial surfaces of the F_1 folds. Unlike the third mode there was no hinge replace-

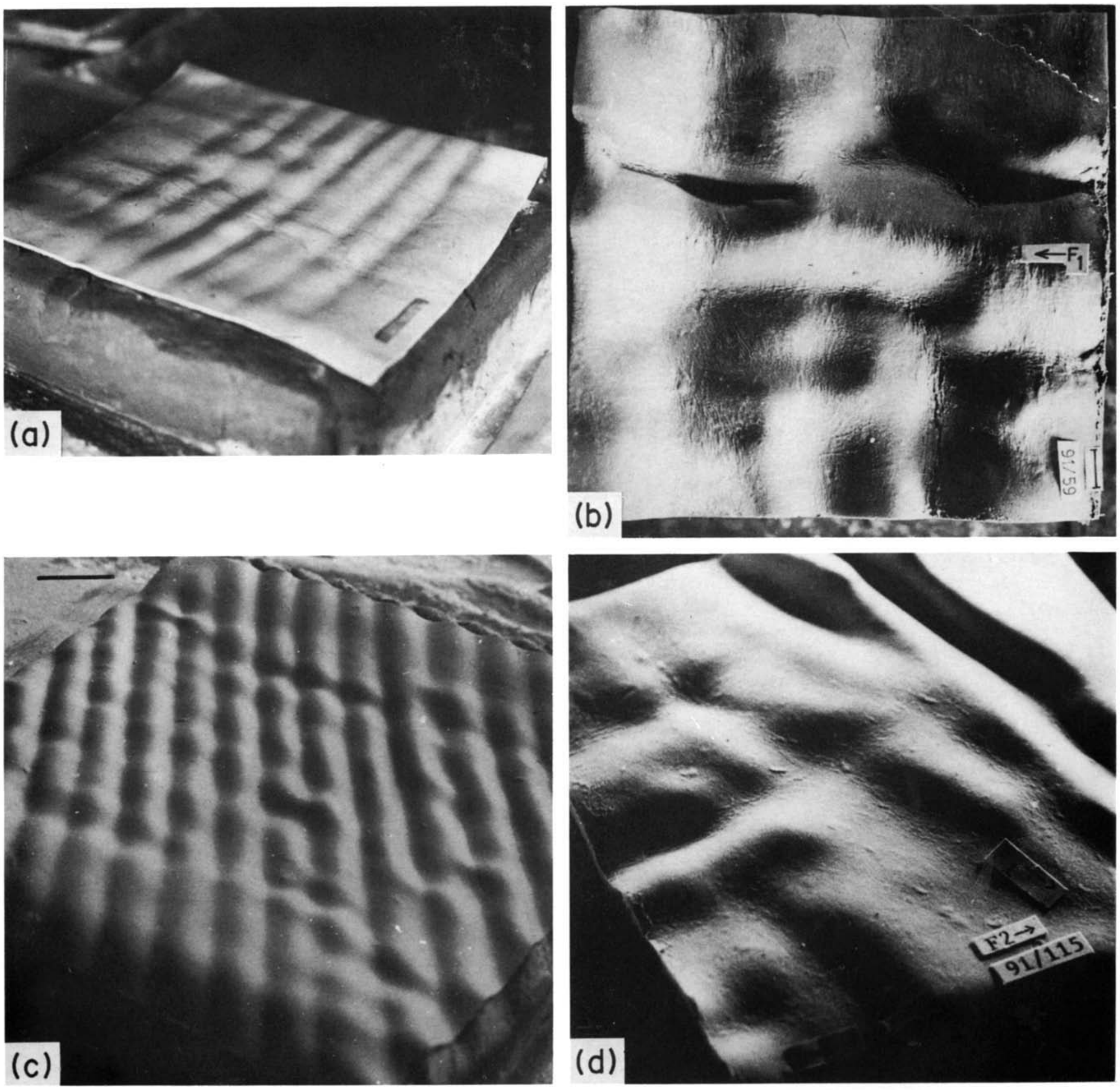

Fig. 2. Gentle dome-and-basin structures in the first mode of superposed buckling. (a) Artificially induced F_1 (parallel to 3 cm long scale on the right-hand side). F_2 trending from left to right, P_1 at a right-angle to P_2. (b) Naturally produced F_1. F_1 and F_2 are at right-angles to each other. Scale bar 1 cm. (c) Artificially induced F_1 trending front to back, F_1 and F_2 at an angle of 60°. Scale bar 3 cm. (d) Naturally produced F_1 at an angle of 65° to F_2. Strip marked F_2 measures 1 cm.

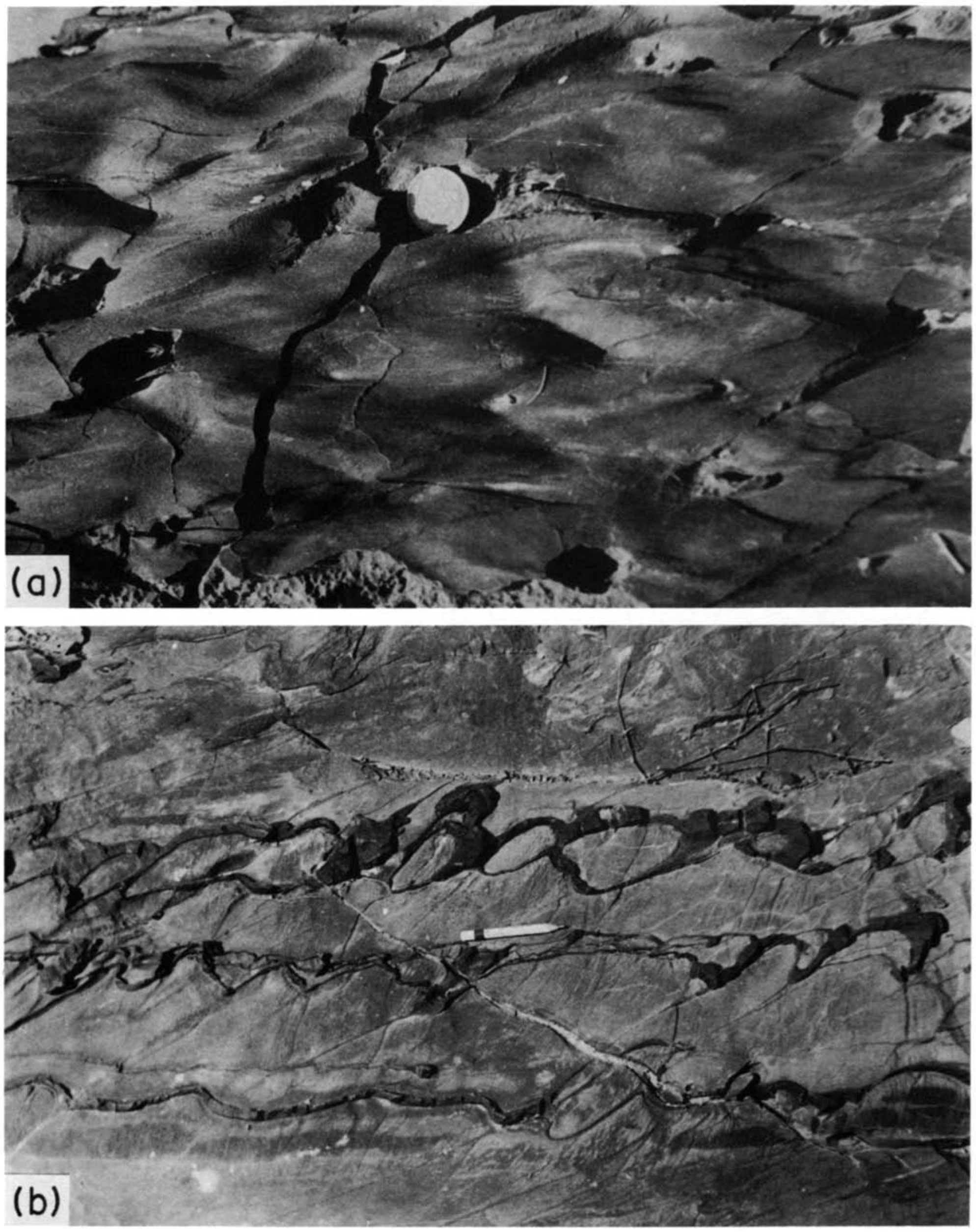

Fig. 3. (a) Dome-and-basin structure formed by the oblique superposition of two generations of open folds in marble–phyllite intercalations; near Narayani temple on the Jaipur–Alwar Road, India. (b) Closed oval outcrops of the first mode of superposed buckling in marble and phyllite intercalations. The long axes of the oval outcrops are oblique to the trends of both sets of folds. Same locality as (a).

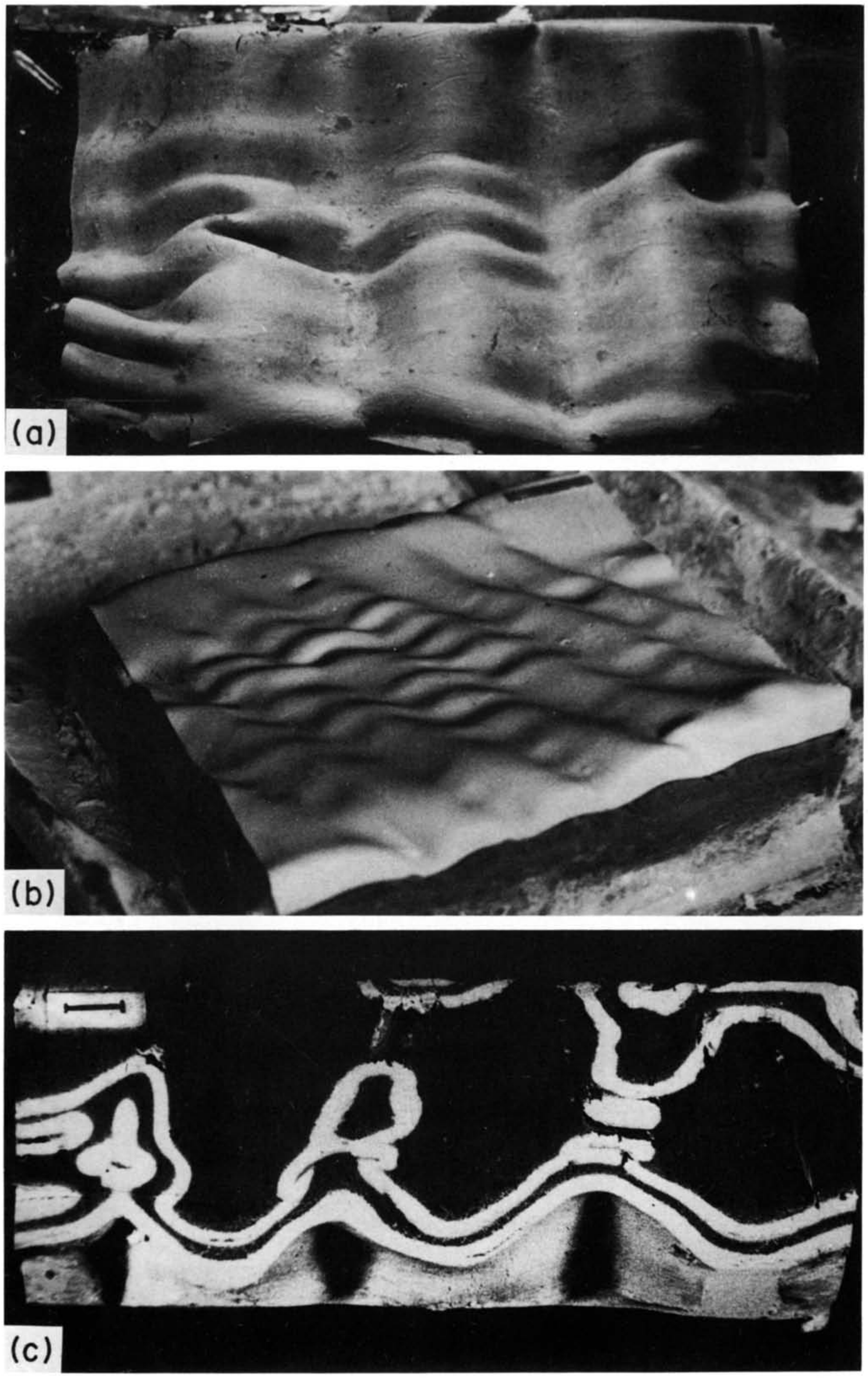

Fig. 4. (a) Second mode of superposed buckling in test model with P_2 at a right-angle to F_1. The F_1 folds trend from front to back and F_2 folds from left to right. (b) Oblique view of model showing superposed buckling in the second mode. The initial angle (θ) between P_2 and F_1 is 30°. Both P_2 and F_1 are horizontal, and the F_2 folds trend from left to right. (c) Outcrop pattern in test model in second mode of superposed buckling. F_1 had an initial plunge of 8° from back to front, and P_2 was horizontal, trending from front to back. Scale bars in (a) and (b) 3 cm long; scale bar in (c) is 1 cm long.

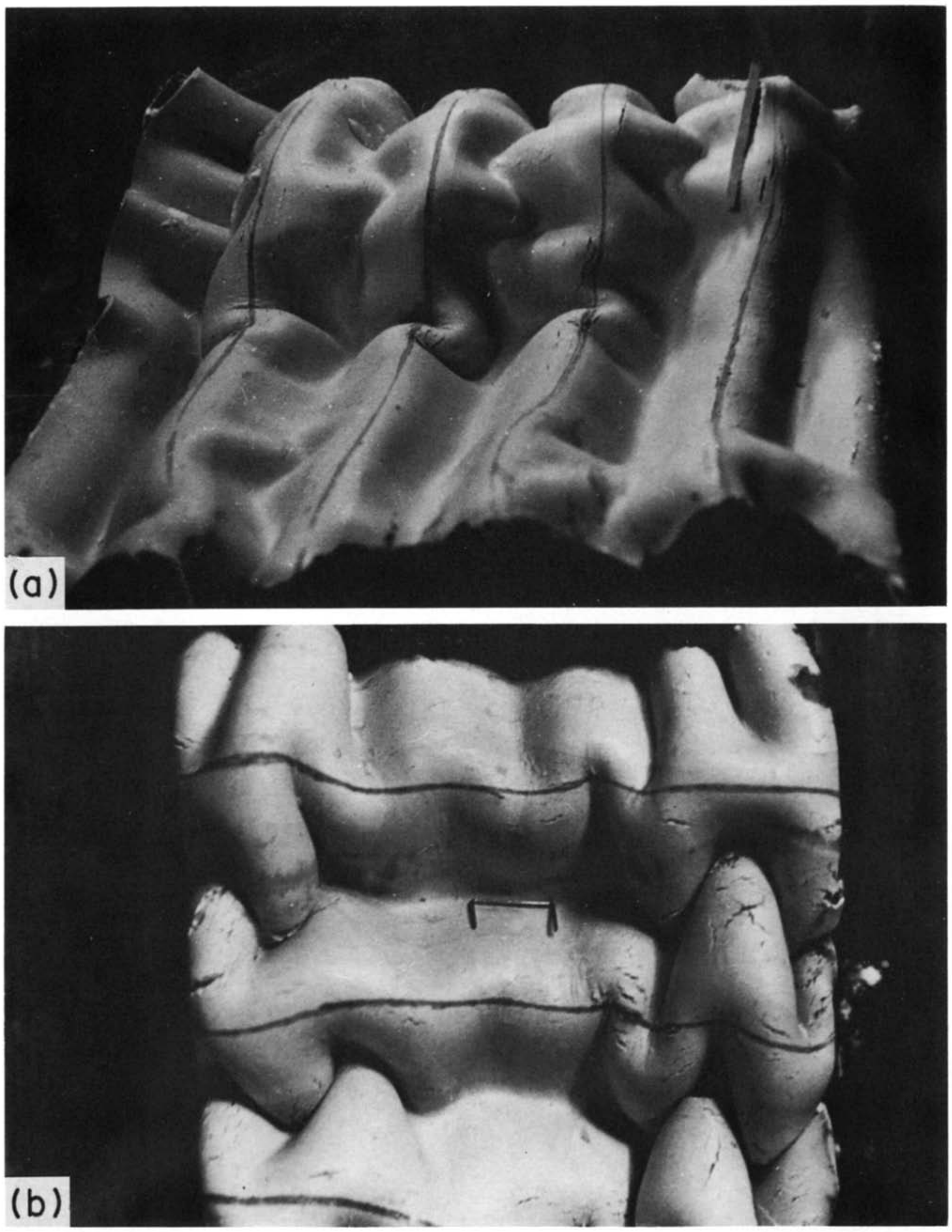

Fig. 5. (a) Third mode of superposed buckling with triangular forms of F_2 antiforms and synforms (with axes trending from left to right). The dark lines mark out the initial hinges of F_1 antiforms. Scale bar 3 cm. (b) Third mode of superposed buckling in test model showing hinge replacement. The dark lines mark out the initial F_1 antiformal hinge lines. These are intersected by the strongly arcuate hinge lines (F_1') of the non-plane folds. The latter are distinct from the hinge lines of F_2 folds (running from top to bottom). With tightening of F_2, the F_1 folds have also become tight. Scale bar 1 cm.

ment or hinge migration for the F_1 folds. If the second deformation involves only a flexure the angle between F_1 and F_2 hinge lines remains constant in different parts of the structure. The angle may not remain constant if the later folding involves both flexure and flattening.

DISCUSSION

Influence of tightness of F_1

This series of experiments shows that the geometry of interference of two generations of buckling folds largely depends on the initial tightness of the early set of folds. With increase in initial tightness of F_1 there is a transition from one mode of superposed buckling to another. Whether superposed buckling takes place according to the first, second, third or fourth modes is decided by both the interlimb angle and the curvature of the folded surface at the hinge zone of F_1. Although on the basis of the experiments we have given a range of F_1 interlimb angles within which a particular mode of superposed buckling was commonly observed, this range is tentative and is modified by the magnitude of curvature of the folded surface at the hinge zone. Thus, for example, in some of the experiments with thick competent layers, the tight F_1 folds had broad and rounded hinges and the smaller F_2 folds of the second mode were localized in the hinge region of F_1. A mixed mode of superposed buckling was noticed in some of the experiments in which the initial tightness of F_1 had a border line value. Thus, when the interlimb angle of F_1 was roughly in the neighbourhood of 135°, the dome-and-basin structure of the first mode was sometimes associated with the second mode structure in which distinctly smaller F_2 folds rode over the hinges of the larger F_1 folds. Similarly, when the F_1 interlimb angle was close to 90° there was, in some of the models, an association of second and third modes of superposed buckling.

In the second mode of superposed buckling, the influence of the magnitude of curvature of the pre-F_2 folded surface on the initial wavelength of the F_2 folds was analysed by Ghosh (1970, pp. 565–567). He considered the development of small second generation folds by axial compression of cylindrical F_1 with semi-circular cusps, and obtained the following relation between the F_2 wavelength and the curvature of F_1 at its hinge zone:

$$(lh)^3 - \frac{6}{n^2 lh} - 6\frac{\mu_1}{\mu_2} = 0, \tag{1}$$

where h is the thickness of the layer, n is the ratio r/h with r as radius of curvature of the middle surface of the layer for the F_1 fold, μ_1 and μ_2 are the coefficients of viscosity of the layer and its embedding medium, and $l = 2\pi/L$, L being the initial wavelength of F_2. If the curvature $1/r$ is 0, this equation gives the dominant wavelength of a cylindrically folded embedded layer (Biot 1957, 1965, p. 423, Ramberg 1964):

$$L_e = 2h\sqrt[3]{\frac{1}{6}\frac{\mu_1}{\mu_2}}. \tag{2}$$

Figure 13 shows the variation of the ratio L_e/L with variation of r/h. The figure shows that with an increase in r/h, L_e/L rapidly decreases and comes very close to 1. Thus, for example, when the viscosity ratio is 50, and $r/h = 13$, $L_e/L = 1.15$. Such a small difference in the arc lengths of F_1 and F_2 means that the dome-and-basin structure will be essentially equant in plan view in the initial stages. These theoretical results do not have a quantitative application in the present case, since, unlike the theoretical model neither the natural nor the experimental F_1 folds have semi-circular cusps. Nevertheless, Fig. 13 suggests that the transition from the first to the second mode may be gradual and not abrupt. If the initial F_1 is very gentle, L_e/L will be close to 1. With a decrease in r/h, when the values of L_e/L become distinctly larger (say >1.5), the second mode of superposed buckling may become noticeable.

Rotation and tightening of plane cylindrical folds in a later deformation

The present series of experiments confirm, in general, the earlier results of Ghosh & Ramberg (1968) that a new set of folds does not develop when the angle between *P*2 and *F*1 is larger than about 30° (i.e. $\alpha = 0$, $\theta > 30°$). There is, however, an exception. In the present experiments, when the initial *F*1 is very gentle, a dome-and-basin pattern did develop when the angle between *P*2 and *F*1 was between 0° and 50°. Apart from this exceptional case, the early folds were always tightened and rotated and a new set of folds did not develop during the second deformation when the angle between *P*2 and *F*1 exceeded about 30°. A similar situation has been described by Naha & Mohanty (1988, p. 86) from southern Rajasthan in India. Here, an E–W longitudinal compression has produced a set of folds with vertical axial planes striking N–S. The *F*2 folds are localized in domains in which the overall orientation of the foliation is steep and has a nearly E–W strike. The *F*2 folds are consistently absent in domains in which the *S*-surfaces strike between NW–SE and N–S. The *F*1 folds in these domains are, instead, further flattened. The presence of such tightened and rotated plane cylindrical folds should be explained as a product of two deformations somewhat similar to the case of redundant superposition of Ramsay & Huber (1987, p. 493), rather than by the localized absence of the later deformation.

Relative tightness of early and late folds

It is a common observation in areas of superposed folding that the earlier folds are tighter than the later folds. Although this is generally true the experiments clearly show that, in the first mode of superposed buckling, a set of tight later folds can be superposed on earlier gentle folds in such a manner that the initial hinge lines

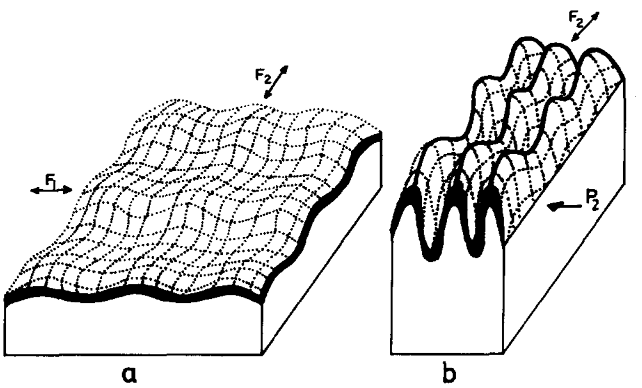

Fig. 6. In the first mode of superposed buckling, when the second shortening (P_2) is very large, the tightening of the F_2 folds is associated with an increase in the curvature of the hinge lines. The hinge lines of the F_1 folds become unrecognizable as in (b).

of the early folds become obliterated and unrecognizable. If both sets of folds are upright, the structure may then show a set of tight or isoclinal, plane F_2 folds with a constant trend and variable and oppositely directed plunge of the fold axes. Here the plunge variation of F_2 axes is the only vestige of the open F_1 folds.

Development of strongly non-cylindrical plane folds

With progressive tightening across the F_2 axial surfaces of a dome-and-basin pattern, and with a large stretching across the general orientation of the layering, the hinge angle (Williams & Chapman 1979) of F_2 decreases and the folds become strongly non-cylindrical. It is conceivable that if the stretching is very large, the structure will evolve into sheath folds. Although the

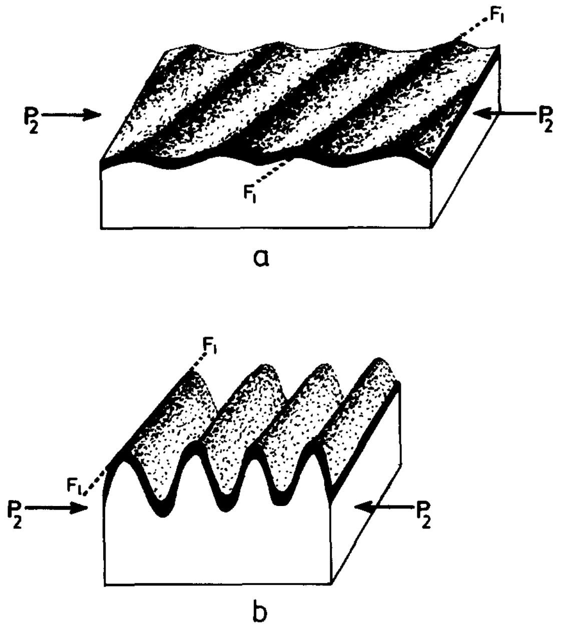

Fig. 7. (a) A set of cylindrical early folds (F_1) undergoing a second period of shortening with the angle between P_2 and F_1 larger than 30°. (b) The F_1 folds are rotated and tightened during the second deformation. Although the folds remain plane cylindrical, their shapes and orientations have been considerably modified by the second deformation. The structure is somewhat similar to the case of redundant superposition of Ramsay & Huber (1987).

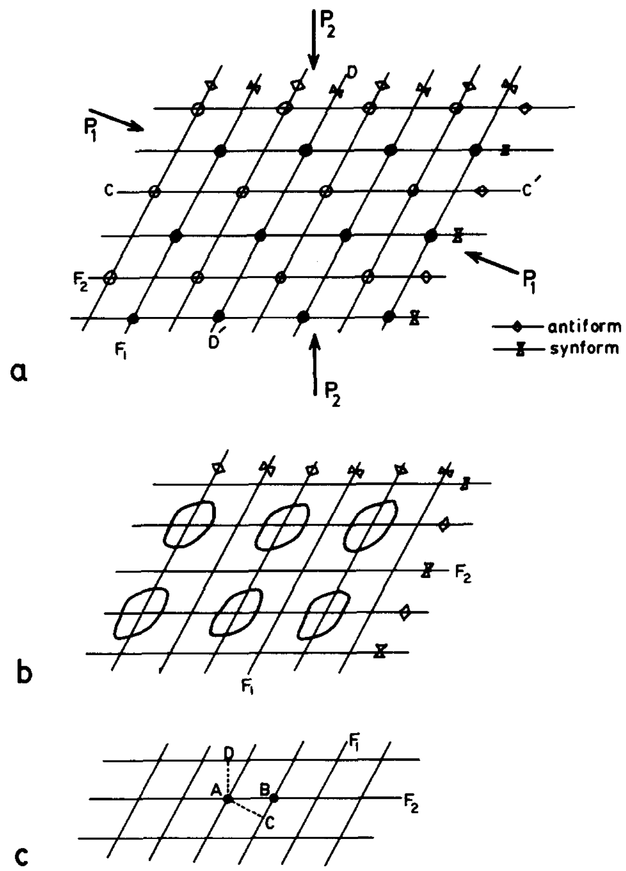

Fig. 8. First mode of superposed buckling with P_2 oblique to F_1. The shortening along P_1 and P_2 are the same. (a) Circles are crest points of domes, dots are trough points of basins. The crests or troughs lie along lines parallel to CC′ at a right-angle to P_2 and along lines DD′ initially at a right-angle to P_1. With progressive tightening of folds during the second deformation the lines parallel to DD′ rotate towards CC′. (b) En échelon oval outcrops with long axes neither parallel to F_1 nor F_2. (c) Although the wavelengths of F_1 and F_2 (AC and AD) are the same, because of oblique superposition the individual domes and basins become elongate. Note that the intercept (AB) of an F_2 fold on an F_1 fold is larger than the wavelength (AC).

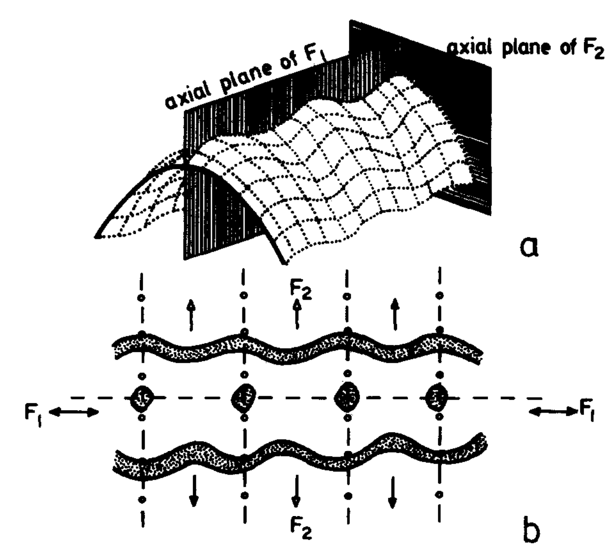

Fig. 9. (a) Second mode of superposed buckling with F_2 at a right-angle to F_1. The smaller F_2 folds ride over the hinge of the larger F_1 fold. (b) Outcrop pattern of second mode of superposed buckling. Dashed line—axial surface trace of F_1; dash-and-dot lines—axial surface traces of F_2.

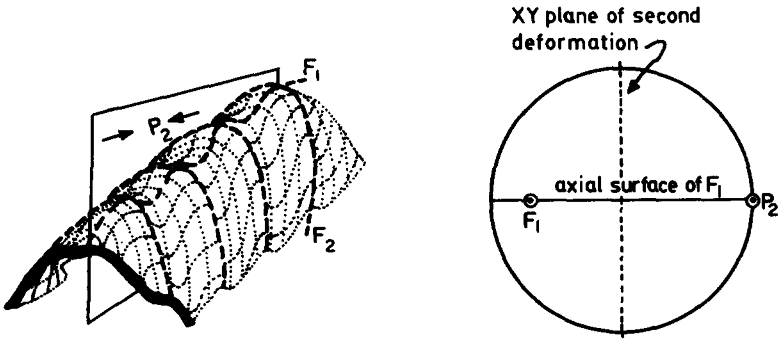

Fig. 10. Second mode of superposed buckling with the direction of second compression (P_2) oblique to F_1. The axial plane of F_1 is vertical. Within it the F_1 axis plunges gently towards the front. The shortening, P_2, is horizontal and is parallel to the axial plane of F_1. The F_1 hinge line is locally distorted by the smaller F_2; its overall orientation is shown in stereographic projection on the right. The F_2 hinge lines show a stronger curvature than that of the initial folded surface of F_1. The diversely oriented hinge lines of F_2 may not lie on a plane.

mechanism of development of sheath folds in a single progressive deformation, as in shear zones or in areas where there is an unequal shortening across the fold axial surfaces (Ramsay 1962, Wood 1974, Ramsay & Huber 1987, fig. 21.33), is fairly well understood, the mechanism of development of sheath folds by interference of two generations of folds (e.g. Turner & Weiss 1963, p. 143, Tobisch 1966, Mukhopadhyay & Sengupta 1979, Skjernaa 1990) has not been studied in detail. As the present experiments indicate, such strongly non-cylindrical plane folds may develop by the flattening of an open dome-and-basin structure, but the strongly

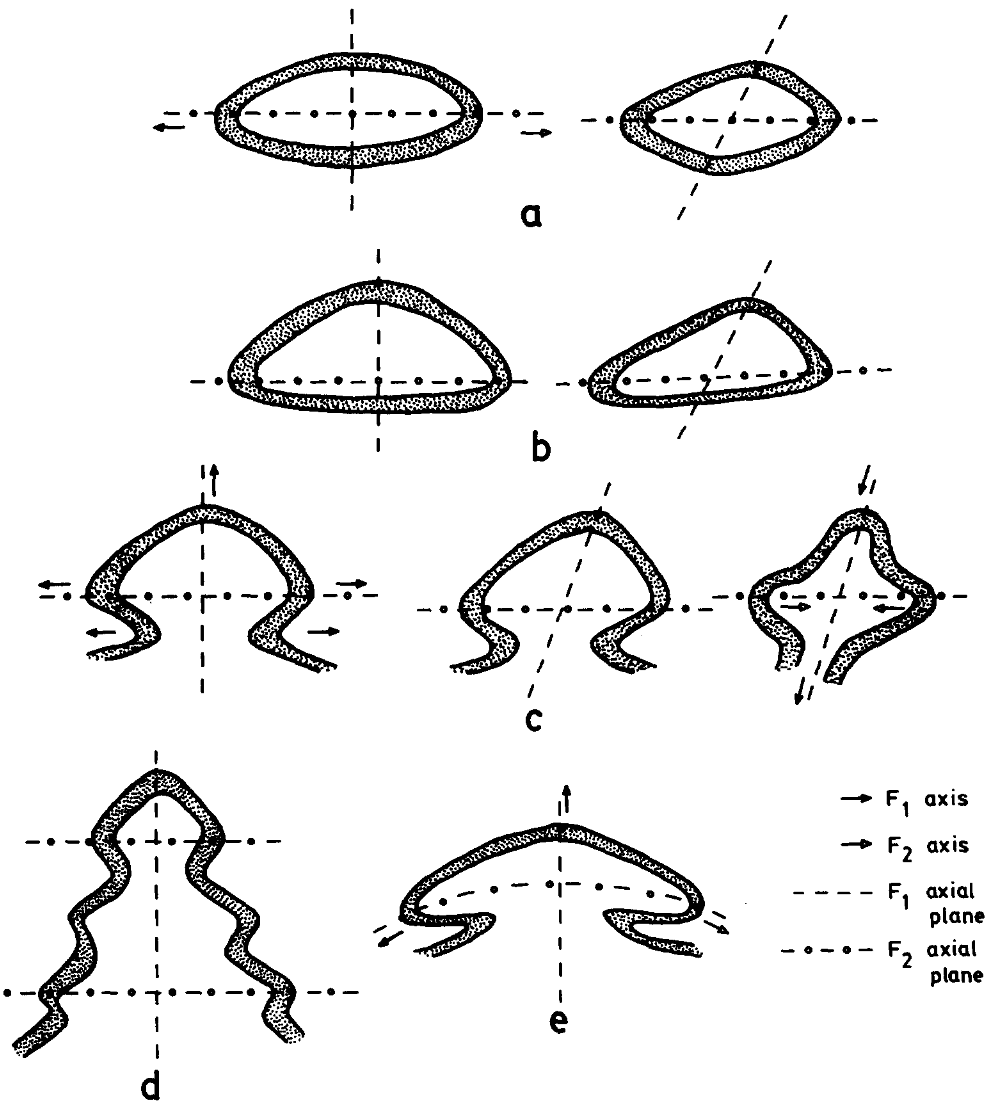

Fig. 11. Outcrop patterns in the second mode of superposed buckling. The axial surfaces of F_1 and F_2 are planar in all cases except in (e) in which the relation between P_2 and F_1 is as in Fig. 10. Sketched from horizontal sections of test models.

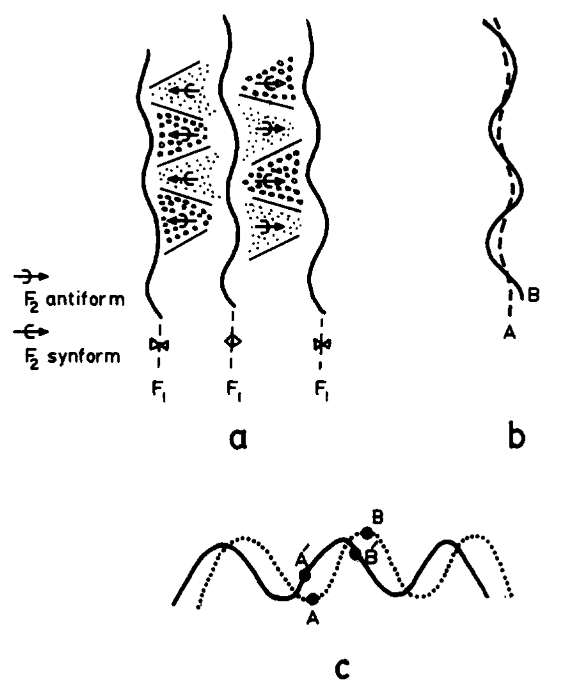

Fig. 12. (a) Plan view of the third mode of superposed buckling. The F_2 antiforms (dotted areas) taper towards the synformal hinges of F_1, and the F_2 synforms (circle-marked areas) taper towards the antiformal hinges of F_1 (b) Dashed line A: gently curved marker line which was initially parallel to an F_1 hinge. Continuous line B: strongly sinuous hinge (F_1') which replaces the F_1 hinge. (c) Dotted line: initial profile of F_1 fold. Continuous line: same profile after the second deformation. The material points A and B have now been shifted to A′ and B′.

curved well-defined hinge line of the structure must belong to F_2. From the experiments it becomes quite clear that, in sharp contrast with the model of shear folding, strongly non-cylindrical plane folds cannot develop by the buckling of a set of tight or isoclinal cylindrical folds; a shortening along their axial planes invariably produces a set of non-plane folds.

Hinge replacement

A remarkable feature of the present series of experiments is the process of hinge replacement in the third mode of buckling (Figs. 5a & b). The term 'hinge replacement' has been used here in preference to the term 'hinge migration' because the process of hinge replacement is associated with only the third mode of superposed buckling. In contrast, hinge migration may take place even during the growth of a set of cylindrical folds. The first and the second modes of superposed buckling can be easily distinguished from their morphology alone. On the other hand, the third and the fourth modes are difficult to distinguish from fold morphology. During the experiments they were mainly distinguished on the basis of whether there was hinge replacement or not. In the experiments this was possible because marker lines were drawn along the initial hinge lines of F_1. During the third mode of superposed buckling a newly created curved hinge line (F_1') was more sinuous than, and was oblique to, the marker line which initially coincided with the F_1 hinge. In natural superposed folds the third mode may be recognized if there is a lineation parallel to F_1. This lineation should be oblique to the newly created sinuous hinge line of F_1'. An important consequence of hinge replacement is that an S_1 cleavage, axial planar to F_1, may be oblique to the hinge lines and axial surfaces of F_1'. Since F_1 hinges are obliterated and are replaced by F_1' hinges, it may appear that S_1 is synchronous with F_1'. S_1 may then appear as a transecting cleavage or non-axial planar cleavage (Stringer & Treagus 1980, Treagus & Treagus 1981). The third mode of superposed buckling may also be recognized from the tapering shapes of the F_2 folds when they are fairly open. This mode of superposed buckling develops only when the F_1 folds are not very tight (i.e. close folds of Fleuty 1964). However, when the F_2 folds superposed on them become isoclinal the F_1 folds are also tightened (Figs. 5b and 14) and may become isoclinal in the major part of the structure. From the fold morphology alone, this tightening of the early folds during a later deformation can hardly be distinguished from the refolding of isoclinal folds by the fourth mode of superposed buckling.

A major technical problem in experimental deformation of test models is to reduce the friction between the model and the horizontal base or the vertical walls. Although these interfaces were well lubricated with oil or liquid detergent, the friction often caused a bulging of the model (Figs. 15a & b). Models which showed a large bulging were usually discarded. Besides such friction-generated bulk inhomogeneity, which only gave rise to a half-wave or a single wave as in Figs. 15(a) & (b), the present series of experiments never gave rise to a train of regular F_2 folds (Fig. 15c) by the buckling of a set of smaller F_1 folds in a type 1 interference on a single competent layer.

The present study is restricted to the problem of superposed buckling in single layers. The experimentally produced F_1 folds did not show a wide range in variation in profile-shapes. They never showed the geometry of chevron folds, conjugate folds or cuspate folds. Moreover, the viscosity contrast between the modelling clay and painter's putty was never extremely large, so that fan folds or elasticas did not develop in the experiments. The viscosity ratio between the modelling clay and the painter's putty was kept more or less the same in the majority of experiments. In one experiment the viscosity ratio was significantly lowered and in another experiment it was increased. The results of these two experiments were in agreement with those obtained from the other experiments. In two experiments, the layer of modelling clay was sandwiched between two slabs of painter's putty (Table 1). The mode of superposed buckling in each of these models was the same as in the models with a free upper surface of the layer of modelling clay having a similar interlimb angle of F_1. The F_1 folds in all the experiments were symmetrical, single-hinged and approximately parallel folds in which the radius of curvature at the hinge and the ratio of hinge zone and fold limb (Ramsay 1967, p. 349) decreased with progressive shortening.

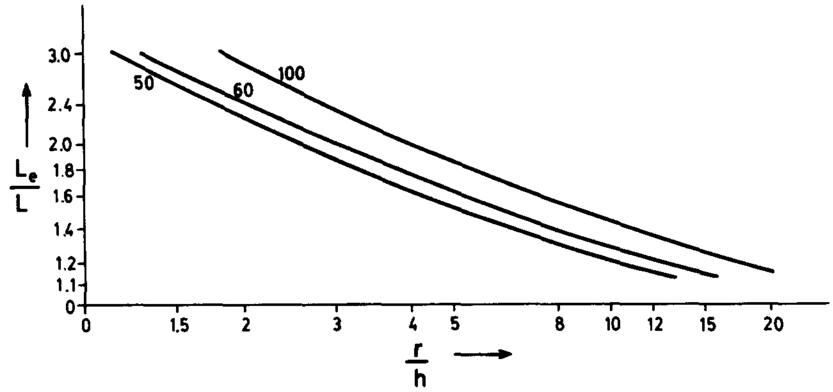

Fig. 13. Natural logarithmic plot of L_e/L against r/h for the second mode of superposed buckling for $\mu_1/\mu_2 = 100, 60$ and 50. L is the wavelength of the non-cylindrical F_2 folds. L_e is the initial wavelength of buckling of a straight embedded layer of the same thickness.

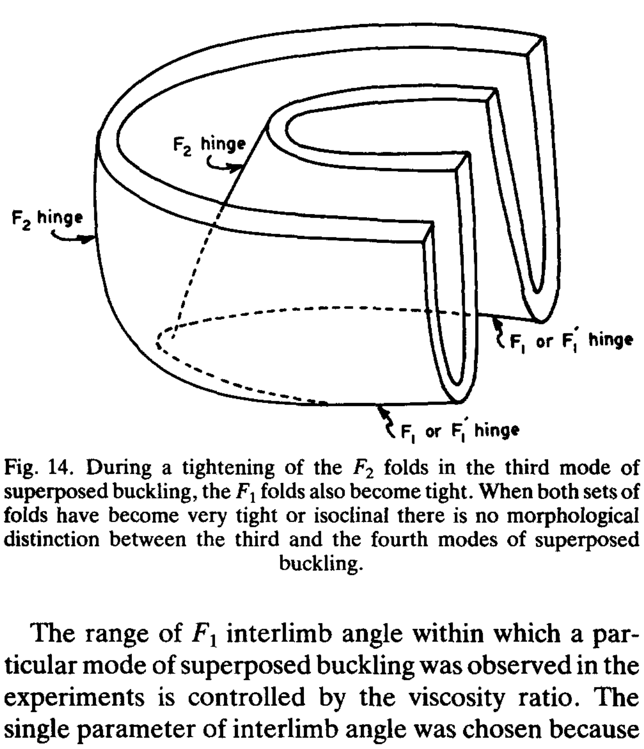

Fig. 14. During a tightening of the F_2 folds in the third mode of superposed buckling, the F_1 folds also become tight. When both sets of folds have become very tight or isoclinal there is no morphological distinction between the third and the fourth modes of superposed buckling.

The range of F_1 interlimb angle within which a particular mode of superposed buckling was observed in the experiments is controlled by the viscosity ratio. The single parameter of interlimb angle was chosen because the interlimb angle could be measured with sufficient accuracy. It is likely that there are other parameters, such as the nature of variation of the curvature along the F_1 fold arc, which influence the mode of superposed buckling. The mechanical aspects of superposed buckle-folding are extremely complex and little understood as yet. In the absence of a theory about the mechanics of superposed buckling it is hardly possible to identify a complete spectrum of F_1 fold shapes that give rise to a particular mode of superposed buckling. Nevertheless, we believe that unless the viscosity ratio is so large that a round-hinged fan fold or an elastica can develop at a large shortening, the observed ranges of the F_1 interlimb angle for the different buckling modes can serve as a first approximation. The major emphasis of the present work is on the recognition of the four modes of superposed buckling in single layers and on the transition from one mode to another with increasing buckle-shortening of the initial F_1.

The profile shapes of cylindrical buckling folds have a much wider range of variations in multilayers than in single layers. Thus, for example, structures similar to that shown in Fig. 15(c) can develop under certain conditions during superposed buckling of multilayers. Moreover, depending upon the profile shape of F_1, the four standard modes of superposed buckling, as described above, may be modified in multilayers. Such complications will be discussed in detail in a later publication.

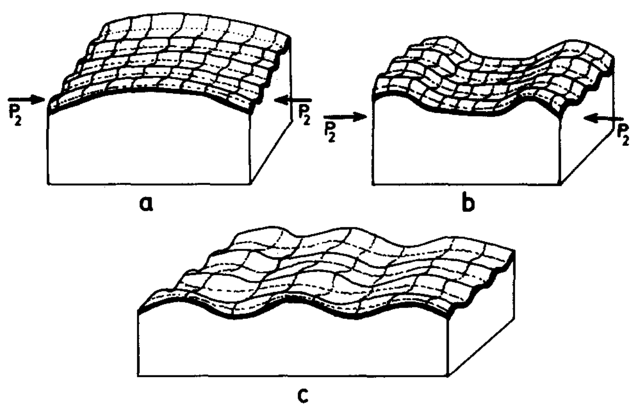

Fig. 15. (a) & (b) Bulging of the model during the second deformation. During superposed buckling of a single layer, small F_1 folds were not refolded to form a number of large F_2 waves as shown in (c).

Acknowledgements—This work was supported by the Council of Scientific and Industrial Research, India. The authors are grateful for the constructive criticisms of Lilian Skjernaa, Peter Hudleston and an anonymous reviewer.

REFERENCES

Biot, M. A. 1957. Folding instability of a layered viscoelastic medium under compression. *Proc. R. Soc. Lond.* **A242**, 444–454.

Biot, M. A. 1965. *Mechanics of Incremental Deformations.* John Wiley & Sons, New York.

de Sitter, L. U. 1952. Plissement croisé dans le Haut-Atlas. *Geol. Mijnb.* **14**, 277–282.

Fleuty, M. J. 1964. The description of folds. *Proc. Geol. Ass.* **75**, 461–492.

Ghosh, S. K. 1970. A theoretical study of intersecting fold patterns. *Tectonophysics* **9**, 559–569.

Ghosh, S. K. & Ramberg, H. 1968. Buckling experiments on intersecting fold patterns. *Tectonophysics* **5**, 89–105.

Julivert, M. & Marcos, A. 1973. Superimposed folding under flexural conditions in the Cantabrian zone (Hercynian Cordillera, northwest Spain). *Am. J. Sci.* **273**, 353–375.

Mukhopadhyay, D. & Sengupta, S. 1979. "Eyed folds" in the Precambrian marbles from southeastern Rajasthan, India. *Bull. geol. Soc. Am.* **90**, 397–404.

Naha, K. & Mohanty, S. 1988. Response of basement and cover rocks to multiple deformation: a study from the Precambrian of Rajasthan, western India. *Precambrian Res.* **42**, 77–96.

Ramberg, H. 1964. Selective buckling of composite layers with contrasted rheological properties: a theory for simultaneous formation of several orders of folds. *Tectonophysics* **1**, 307–341.

Ramsay, J. G. 1962. The geometry and mechanics of formation of "similar" type folds. *J. Geol.* **70**, 309–327.

Ramsay, J. G. 1967. *Folding and Fracturing of Rocks*. McGraw-Hill, New York.

Ramsay, J. G. & Huber, M. I. 1987. *The Techniques of Modern Structural Geology, Volume 2: Folds and Fractures*. Academic Press, London.

Skjernaa, L. 1975. Experiments on superposed buckle folding. *Tectonophysics* **27**, 255–270.

Skjernaa, L. 1990. Tubular folds and sheath folds: definitions and conceptual models for their development, with examples from Grapesvara area, northern Sweden. *J. Struct. Geol.* **11**, 689–703.

Stringer, P. & Treagus, J. E. 1980. Non-axial planar S_1 cleavage in the Hawick Rocks of the Galloway area, Southern Uplands, Scotland. *J. Struct. Geol.* **2**, 317–331.

Timoshenko, S. P. & Gere, J. M. 1961. *Theory of Elastic Stability*. McGraw-Hill, New York.

Tobisch, O. T. 1966. Large scale basin and dome pattern resulting from the interference of major folds. *Bull. geol. Soc. Am.* **77**, 415–419.

Treagus, J. E. & Treagus, S. H. 1981. Folds and the strain ellipsoid: a general model. *J. Struct. Geol.* **3**, 1–17.

Turner, F. J. & Weiss, L. E. 1963. *Structural Analysis of Metamorphic Tectonites*. McGraw-Hill, New York.

Watkinson, A. J. 1981. Patterns of fold interference: influence of early fold shapes. *J. Struct. Geol.* **3**, 19–23.

Williams, G. D. & Chapman, T. J. 1979. The geometrical classification of noncyclindrical folds. *J. Struct. Geol.* **1**, 181–185.

Wood, D. S. 1974. Current views of the development of slaty cleavage. *Annu. Rev. Earth & Planet. Sci.* **2**, 369–401.